Published in final edited form as:
Magn Reson Med. 2007 October ; 58(4): 850–854. doi:10.1002/mrm.21388.

Very-Low-Frequency Electron Paramagnetic Resonance (EPR) Imaging of Nitroxide-Loaded Cells

Joseph P.Y. Kao[1,4,5,*], **Eugene D. Barth**[2,6], **Scott R. Burks**[1,4,5], **Philip Smithback**[2,6], **Colin Mailer**[2,6], **Kang-Hyun Ahn**[2,6], **Howard J. Halpern**[2,6], and **Gerald M. Rosen**[1,3,5]

[1]Medical Biotechnology Center, University of Maryland Biotechnology Institute, Baltimore, Maryland, USA

[2]Department of Radiation and Cellular Oncology, University of Chicago, Chicago, Illinois, USA

[3]Department of Pharmaceutical Sciences, University of Maryland School of Pharmacy, Baltimore, Maryland, USA

[4]Department of Physiology, University of Maryland School of Medicine, Baltimore, Maryland, USA, Baltimore, Maryland, USA

[5]Center for EPR Imaging In Vivo Physiology, University of Maryland, Baltimore, Maryland, USA

[6]Center for EPR Imaging In Vivo Physiology, University of Chicago, Chicago, Illinois, USA

Abstract

Recent advances in electron paramagnetic resonance (EPR) imaging have made it possible to image, in real time in vivo, cells that have been labeled with nitroxide spin probes. We previously reported that cells can be loaded to high (millimolar) intracellular concentrations with (2,2,5,5-tetramethylpyrrolidin-1-oxyl-3-ylmethyl)amine-*N*,*N*-diacetic acid by incubation with the corresponding acetoxymethyl (AM) ester. Furthermore, the intracellular lifetime ($t_{1/e}$) of this nitroxide is 114 min—sufficiently long to permit in vivo imaging studies. In the present study, at a gradient of ~50 mT/m, we acquire and compare EPR images of a three-tube phantom, filled with either a 200-μM solution of the nitroxide, or a suspension of cells preincubated with the nitroxide AM ester. In both cases, 3-mm resolution images can be acquired with excellent signal-to-noise ratios (SNRs). These findings indicate that cells well-loaded with nitroxide are readily imageable by EPR imaging, and that in vivo tracking studies utilizing such cells should be feasible.

Keywords

nitroxide; EPR imaging; persistent nitroxide; cellular imaging; nitroxide imaging; radio frequency EPR

The ability to label a specific cell type and image its movement in vivo, noninvasively and in real time would be of great importance in understanding the interactions of cells that regulate a spectrum of human physiology and in the diagnosis and evaluation of human diseases. Potential uses include tracking the migration of lymphocytes in autoimmune-related diseases such as multiple sclerosis (1,2), or monitoring the accumulation of immune cells at a site of tissue graft (3,4) or at loci of inflammation (5). Longer term imaging of tumor cells could, likewise, permit long-term studies of metastases (6).

---

[*]Correspondence to: Joseph P.Y. Kao, Medical Biotechnology Center, University of Maryland Biotechnology Institute, 725 W. Lombard St., Baltimore, MD 21201. jkao@umaryland.edu.

In recent years, magnetic resonance imaging (MRI) with contrast media has been used to study a variety of important physiological processes (3,7–11). However, with the development of low-frequency electron paramagnetic resonance (EPR) spectrometers capable of detecting paramagnetic species in living animals in real time (12–16), EPR imaging is now an alternative technology that can, like MRI, address significant physiological questions. The challenge, however, has been the synthesis of paramagnetic spin probes that can provide these essential data. A trityl radical, for instance, has been employed to image O_2 in solid tumors in vivo by EPR (17). Being large and highly charged molecules, the trityl radicals cannot readily diffuse into cells; therefore, the utility of this paramagnetic probe is limited to extracellular measurements.

Because of their chemical flexibility, ease of preparation, and stability at physiological temperature and pH, nitroxides are well-suited for cellular imaging applications. For example, high intracellular concentration of nitroxide has been attained by entrapping the anion of 3-carboxy-2,2,5,5-tetramethyl-1-pyrrolidinyloxyl [1] in lymphocytes by incubation with its membrane-permeant precursor 3-acetoxymethoxycarbonyl-2,2,5,5-tetramethyl-1-pyrrolidinyloxyl [2] (18). The membrane-permeant nitroxide [2] passively enters the cytosol, where it is hydrolyzed by intracellular esterases to yield the membrane-impermeant anionic nitroxide [1] (Fig. 1a), which can accumulate intracellularly to millimolar concentrations. Although nitroxide [1] is highly resistant to bioreduction, it is rapidly extruded from lymphocytes by organic anion transporters (19). This finding suggested that an analog of nitroxide [1] bearing both positive and negative charges might be better retained in these cells. Toward this goal, we synthesized (2,2,5,5-tetramethylpyrrolidin-1-oxyl-3-ylmethyl)amine-*N,N*-diacetic acid diacetoxymethyl ester [3], which is converted by intracellular esterase hydrolysis to (2,2,5,5-tetramethylpyrrolidin-1-oxyl-3-ylmethyl)amine-*N,N*-diacetate [4], which also accumulates intracellularly to millimolar levels (19). At physiologic pH, nitroxide [4] carries two negative charges and one positive charge (Fig. 1b). We found that the highly-charged nature of nitroxide [4] greatly enhanced its retention in lymphocytes: the intracellular retention lifetime was $t_{1/e}$ = 114 min at 37°C (19).

In the present study, we report EPR imaging of lymphocytes that have intracellularly entrapped nitroxide [4]. The images show a resolution of 3 mm, sufficient to monitor and localize cell populations.

MATERIALS AND METHODS

Chemicals

Nitroxides, (2,2,5,5-tetramethylpyrrolidin-1-oxyl-3-ylmethyl)-amine-*N,N*-diacetic acid diacetoxymethyl ester [3] and (2,2,5,5-tetramethylpyrrolidin-1-oxyl-3-ylmethyl) amine-*N,N*-diacetic acid [4] were synthesized as described previously (19) (see Fig. 1b for structures). For cell studies, a 40-mM stock solution of nitroxide [3] in dimethylsulfoxide was prepared. For cell loading, the stock solution was diluted to 40 μM in Roswell Park Memorial Institute (RPMI) 1640 medium.

Construction of Phantom for Low-Frequency EPR Imaging

The imaging phantom is illustrated in Fig. 2 and comprised three identical glass tubes, each with an inner diameter of 4.71 mm and an outer diameter of 7.01 mm. With their long axes aligned in parallel, the tubes were bundled in an equilateral triangular arrangement. Each tube received ~200 μl of sample, which spanned ~11.5 mm of the length of the tube. Plugs fabricated from hydrophilic polyvinylsiloxane dental impression material (GC Dental Products, Kasugai, Japan) were placed at the two ends of each tube, to fix the sample in the

middle. To stabilize the triangular geometry, the tubes were placed in a precast cylindrical polyvinylsiloxane mold.

Low-Frequency EPR Imaging of a Nitroxide Solution

Each tube in the phantom was filled with a solution of nitroxide [4] (200 μM) and the phantom was positioned in the approximate center of the resonant cavity of a 250-MHz EPR imaging spectrometer. The resonator was a loop-gap resonator with single loop and a single gap. The sample holding loop was 16 mm in diameter and 15 mm deep. With a single tube of cells, its loaded Q was 275, and with three tubes, the loaded Q was 200. A 0.36-mT spectral window encompassed the central spectral peak of the nitroxide [4]. Other instrumental parameters were: power, 16 mW; modulation amplitude and frequency, 0.137 mT and 4.980 kHz, respectively; lock-in time constant, 30 ms, with a 30 ms per point dwell time; 256 points per projection; field gradient, 50.3 mT/m. For an X-Z image, acquisitions were made at 99 polar angles in ~15 min.

The natural Lorentzian line width of approximately 80 mG of the central line of nitroxide [4] in the phantom was broadened by unresolved hyperfine splittings of approximately 0.2 and 0.5 G from methyl and axial protons, respectively, to produce a peak-to-peak width of 1.3 G. These parameters in the individual manifold were extracted using the algorithm of Robinson et al. (20), which fully accounts for the modulation frequency and amplitude.

At 250 MHz, the Breit-Rabi term in the hyperfine splitting is large, so that the center of the manifold with the z-component of the nitrogen nuclear spin equal to zero ($m_z = 0$) is shifted downfield from the position midway between the downfield ($m_z = 1$) and upfield ($m_z = -1$) manifolds. This is evident in the unequal spacings of the three lines in the spectrum obtained at 264.4 MHz (Fig. 3). The splitting between the downfield and central manifolds is 14.506 G, whereas that between the central and upfield manifolds is 17.298 G. Using these line separations, we can evaluate the high-field splitting to be 15.5 G (21).

Loading of Lymphocytes With Nitroxide [3]

Jurkat lymphocytes (gift of Dr. Alfredo Garzino Demo, University of Maryland Biotechnology Institute) were maintained in bicarbonate-buffered RPMI 1640 medium (Biofluids, Rockville, MD, USA) supplemented with 100 U/ml penicillin (Gibco, Grand Island, NY), 100 μg/ml streptomycin (Gibco), 2 mM L-glutamine (Gibco), and 10% v/v fetal bovine serum (FBS; Atlanta Biologicals, Law-renceville, GA, USA). For loading with nitroxide [3], cells were suspended in the medium described above from which FBS was omitted. This loading medium also contained nitroxide [3] (40 μM) and 0.0015% w/v Pluronic F-127 surfactant (BASF Corp., Washington, NJ, USA). The cell suspension (2.2×10^6 cells/ml) was incubated on a rocker at room temperature for 70 min, at which point the cell suspension was centrifuged for 3.5 min at 1000 rpm. The cells were washed by resuspending the pellet in RPMI 1640 medium containing 10% v/v FBS and again centrifuged at 1000 rpm. This washing procedure was repeated two more times. The final cell pellet was resuspended in Hanks' Balanced Salt Solution (HBSS; Gibco) for EPR imaging experiments.

Low-Frequency EPR Imaging of Nitroxide-Loaded Lymphocytes

The loaded cells suspended in HBSS were transferred into the phantom, with each tube receiving ~200 μl of cell suspension, containing 2.6×10^7 cells. The spectral window was 0.5 mT; all other parameters were the same as for imaging of the nitroxide solution. For a three-dimensional (3D) image, 100 projections (10 polar projections, each with 10 azimuthal projections) were acquired in ~15 min for image reconstruction. For nitroxide [4] loaded in cells, the natural Lorentzian line width of the central line of approximately 0.5 G was

broadened by unresolved hyper-fine splittings of approximately 0.2 and 0.5 G from the methyl and axial protons, respectively, to produce a peak-to-peak width of 1.5 G. The broadened Lorentzian is presumably due to an increased rotation correlation time of the nitroxide caused by the greater viscosity of the intra-cellular environment.

Data Processing and Image Reconstruction

Continuous wave (CW) EPR intensity images were obtained using a tomographic technique. A total of 99 projections, defined as field-swept CW spectra in the presence of a 50.3 mT/m gradient whose direction was oriented perpendicular to the long axis of the sample tube, were obtained in ~8 s, with 256 points uniformly spaced in the magnetic field and a point dwell time of 30 ms. A filtered back-projection algorithm was used for image reconstruction (22). Projections were filtered using a simple cutoff of the image response frequency to half the Nyquist sampling limit. Images were reconstructed without correction for the effect of the two other spectral lines not included in the spectral window of 0.36 mT or 0.5 mT. Since the manifold splittings were greater than 14 G (1.4 mT), there was no artifact or sacrifice in resolution.

Spatial resolution of an imaging system is commonly defined by the full-width at half-maximum (FWHM) of a point spread function (PSF). Three synthesized discs reproducing the geometry of the phantom were convolved with a two-dimensional (2D) Gaussian PSF to model the imaging process. Subtraction of the EPR image from the synthetic image yielded minimum residual when the FWHM of the PSF was 3 mm.

The signal-to-noise ratio (SNR) for the phantom containing nitroxide solution was determined by selecting a region of the image including only signal and evaluating the mean value of the pixels from this region. A region with the same number of pixels outside the signal was selected and the standard deviation of its “signal” was computed. Taking the ratio of the signal mean to the SD outside the signal gave a value of 125 for the SNR. The SNR for the phantom containing nitroxide-loaded cells was 100–140, determined as the ratio of the root-mean-square (RMS) height of the signal to the RMS value of the baseline. The variation was largely due to baseline drift, which caused the “noise” to be artificially high.

RESULTS

Presented in Fig. 4 is a 2D EPR image in the X-Z plane of the phantom, which shows the cross-sections of the three cylinders each filled with an aqueous solution of nitroxide [4] (200 μM). The image was reconstructed from data obtained by taking one spectral projection along each of 99 azimuthal angles in the X-Z plane. Three distinct red circular regions of high intensity are visible on a pseudocolor scale, where blue is the lower limit value, and red the upper limit value. The known geometry and dimensions of the phantom are clearly reflected in the nitroxide image where the diameter of each circular signal matches that of each tube’s inner diameter. As well, spaces separating the red discs faithfully represent the thickness of the glass tubing in the phantom. The yellow rings about the relatively uniform nitroxide concentration represent partial volume averaging due to finite resolution of the image, and a sharp transition from maximal signal in the nitroxide solution to zero signal in the glass.

Figure 5a shows a view of the phantom identical to that of Fig. 4, but instead of an aqueous solution of nitroxide [4], each tube contains 2.6×10^7 lymphocytes that have been preincubated with nitroxide [3] to enable intracellular accumulation of nitroxide [4]. Unlike the 2D image in Fig. 4, which was reconstructed from 99 azimuthal projections in the X-Z plane, the image in Fig. 5a is an X-Z section through a 3D image reconstructed from scans of 100 total projections (10 polar angles, each with 10 azimuthal angles). While there is

some degradation in image quality, the spatial information derived from this image is essentially identical to that in Fig. 4. Shown in Fig. 5b are two X-Y sections through the same 3D reconstruction. The two sections are taken at positions in the phantom marked by lines A and B in Fig. 2. Again, the dimensions of the phantom are well represented in the reconstructed image. Some geometric irregularities are apparent, and are attributable to sedimentation of lymphocytes within the glass tubes during the course of data collection.

DISCUSSION

We have shown that it is possible to obtain very low-frequency EPR images of an intracellularly-trapped nitroxide with excellent sensitivity and 3-mm resolution. Although the EPR images shown in Fig. 5 do not differentiate between intracellular and extracellular nitroxide, from previous kinetic studies (19), we estimate that greater than 90% of nitroxide [4] is retained within the lymphocytes. This finding validates the possibility of monitoring cell populations in vivo: once retained intracellularly, the nitroxides “tag” the cells, allowing their position and movement throughout the body to be monitored by EPR imaging.

This work describes a proof-of-principle that nitroxides confined within cells are imageable by EPR imaging. To make this technology practical for in vivo EPR imaging over a period of many hours, synthesis of a new family of nitroxides will be required. For instance, intracellular retention time of a nitroxide depends on its ionic character. At physiologic pH, nitroxide [4] bears two negative charges and one positive charge, resulting in net anionic character (Fig. 1b). Nitroxide [4] is retained in lymphocytes with a lifetime of $t_{1/e} = 114$ min at 37°C (19); thus, the signal inside the cells remains measurable for several hours. This is a great improvement over the singly charged nitroxide [1], which has a retention lifetime of only 10 min at 37°C (19). However, future advancement in EPR imaging will require the development of nitroxides with intracellular lifetimes greater than that of nitroxide [4]. Knowing the dependence of intracellular retention on ionic character will enable rational optimization of the nitroxide structure through chemical synthesis.

In the current imaging study we have achieved excellent SNR and 3-mm spatial resolution. However, significant improvements are possible through rational refinement of the nitroxide molecular structure. Hyperfine interactions at the nitrogen (^{14}N) atom causes an otherwise sharp, single resonance to split into three broader peaks, each having one-third the total intensity. In imaging, the height of only a single peak can be measured. Therefore, SNR can be improved by preparing nitroxides containing ^{15}N, which gives rise to two spectral lines, each with half of the total intensity. The result is a 50% increase in the single-peak signal. Hyperfine splitting due to protons broadens each peak in the nitroxide spectrum. The broader peak means resonance occurs over a greater range of magnetic field. This translates into reduced spatial resolution as magnetic field gradients are used for spatial imaging. Because deuterons have much weaker hyperfine interactions than protons, perdeuteration of the nitroxide will sharpen the EPR spectral peaks significantly. In consequence, perdeuteration should improve spatial resolution as well as SNR. The rational improvements outlined above are under way.

The data presented here, in combination with the aforementioned refinement of nitroxide imaging probes, should greatly increase the potential for using EPR imaging to image and track cell populations in vivo. For example, MRI with ultra-small iron oxide particles (USPIO), used as a contrast agent, is being developed to monitor lymphocyte migration to sites of tissue rejection in organ transplant (3,4). These types of studies would be accessible by low-frequency EPR imaging with intracellular nitroxides, as the physiology occurs on a time scale that is entirely compatible with EPR imaging. A major advantage of the present technique is the reduced toxicity and perturbation of the cellular environment by nitroxides

relative to super-paramagnetic iron oxide particles. In addition to cellular localization, the spectra of EPR spin probes can provide unique physiological information about the intracellular environment poorly accessible to MRI. Spectral imaging can measure intracellular oxygen concentration, pH, and viscosity, as the EPR spectra of many spin probes are predictably influenced by these properties. These intracellular measurements are crucial to understanding states of tissue in disease and health.

Acknowledgments

This work was supported in part by grants from the National Institutes of Health: P41-EB-2034 (to G.M.R. and H.J.H.) and GM-56481 (J.P.Y.K.).

References

1. Muraro PA, Wandinger KP, Bielekova B, Gran B, Marques A, Utz U, McFarland HF, Jacobson S, Martin R. Molecular tracking of antigen-specific T cell clones in neurological immune-mediated disorders. Brain. 2003; 126:20–31. [PubMed: 12477694]
2. Markovic-Plese S, McFarland HF. Immunopathogenesis of the multiple sclerosis lesion. Curr Neurol Neurosci Rep. 2001; 1:257–262. [PubMed: 11898527]
3. Ho C, Hitchens TK. A non-invasive approach to detecting organ rejection by MRI: monitoring the accumulation of immune cells at the transplanted organ. Curr Pharm Biotechnol. 2004; 5:551–566. [PubMed: 15579044]
4. Wu YL, Ye Q, Foley LM, Hitchens TK, Sato K, Williams JB, Ho C. In situ labeling of immune cells with iron oxide particles: an approach to detect organ rejection by cellular MRI. Proc Natl Acad Sci USA. 2006; 103:1852–1857. [PubMed: 16443687]
5. Schon MP, Ludwig RJ. Lymphocyte trafficking to inflamed skin—molecular mechanisms and implications for therapeutic target molecules. Expert Opin Ther Targets. 2005; 9:225–243. [PubMed: 15934912]
6. Ottobrini L, Lucignani G, Clerici M, Rescigno M. Assessing cell trafficking by noninvasive imaging techniques: applications in experimental tumor immunology. Q J Nucl Med Mol Imaging. 2005; 49:361–366. [PubMed: 16407819]
7. Atri M. New technologies and directed agents for applications of cancer imaging. J Clin Oncol. 2006; 24:3299–3308. [PubMed: 16829654]
8. Deans AE, Wadghiri YZ, Bernas LM, Yu X, Rutt BK, Turnbull DH. Cellular MRI contrast via coexpresseion of transferring receptor and ferritin. Magn Reson Med. 2006; 56:51–59. [PubMed: 16724301]
9. Thorek DL, Chen AK, Czupryna J, Tsourkas A. Superparamagnetic iron oxide nanoparticle probes for molecular imaging. Ann Biomed Eng. 2006; 34:23–38. [PubMed: 16496086]
10. Mulder WJ, Strijkers GJ, van Tilborg GA, Griffioen AW, Nicolay K. Lipid-based nanoparticles for contrast-enhanced MRI and molecular imaging. NMR Biomed. 2006; 19:142–164. [PubMed: 16450332]
11. Modo M, Hoehn M, Bulte JW. Cellular MR imaging. Mol Imaging. 2005; 4:143–164. [PubMed: 16194447]
12. Halpern, HJ.; Bowman, MK. Low-frequency EPR spectrometers: MHz range. In: Eaton, GR.; Eaton, SS.; Ohno, K., editors. EPR imaging and in vivo EPR. Boca Raton, FL: CRC Press; 1991. p. 45-63.
13. Komarov A, Mattson D, Jones MM, Singh PK, Lai C-S. In vivo spin trapping of nitric oxide in mice. Biochem Biophys Res Comm. 1993; 195:1191–1198. [PubMed: 8216248]
14. Halpern HJ, Yu C, Barth E, Peric M, Rosen GM. In situ detection, by spin trapping of hydroxyl radical markers produced from ionizing radiation in the tumor of a living mouse. Proc Natl Acad Sci USA. 1995; 92:796–800. [PubMed: 7846054]
15. Yoshimura T, Yokoyama H, Fujii S, Takayama F, Oikawa K, Kamada H. In vivo EPR detection and imaging of endogenous nitric oxide in lipopolysaccharide-treated mice. Nat Biotechnol. 1996; 14:992–994. [PubMed: 9631037]

16. Halpern HJ, Peric M, Yu C, Barth ED, Chandramouli GVR, Makinen MW, Rosen GM. In vivo spin-label murine pharmacodynamics using low frequency electron paramagnetic resonance imaging. Biophys J. 1996; 71:403–409. [PubMed: 8804623]

17. Elas M, Williams BB, Parasca A, Mailer C, Pelizzari CA, Lewis MA, River JN, Karczmar GS, Barth ED, Halpern HJ. Quantitative tumor oxymetric images from 4D electron paramagnetic resonance imaging (EPRI): methodology and comparison with blood oxygen level-dependent (BOLD) MRI. Magn Reson Med. 2003; 49:682–691. [PubMed: 12652539]

18. Kao JPY, Rosen GM. Esterase-assisted accumulation of 3-carboxy-2,2,5,5-tetramethyl-1-pyrrolidinyloxyl into lymphocytes. Org Biomol Chem. 2004; 2:99–102. [PubMed: 14737666]

19. Rosen GM, Burks SR, Kohr MJ, Kao JPY. Synthesis and biological testing of aminoxyls designed for long-term retention by living cells. Org Biomol Chem. 2005; 3:645–648. [PubMed: 15703801]

20. Robinson BH, Mailer C, Reese AW. Linewidth analysis of spin labels in liquids. I. Theory and data analysis. J Magn Reson. 1999; 138:199–209. [PubMed: 10341123]

21. Weil, JA.; Bolton, JR.; Wertz, JE. Electron paramagnetic resonance: elementary theory and practical applications. New York: John Wiley & Sons, Inc; 1994. p. 592

22. Barrett, HH. The Radon transformation and its applications. In: Wolf, E., editor. Progress in Optics XXI. Amsterdam: Elsevier Science Publishers; 1984. p. 219-286.

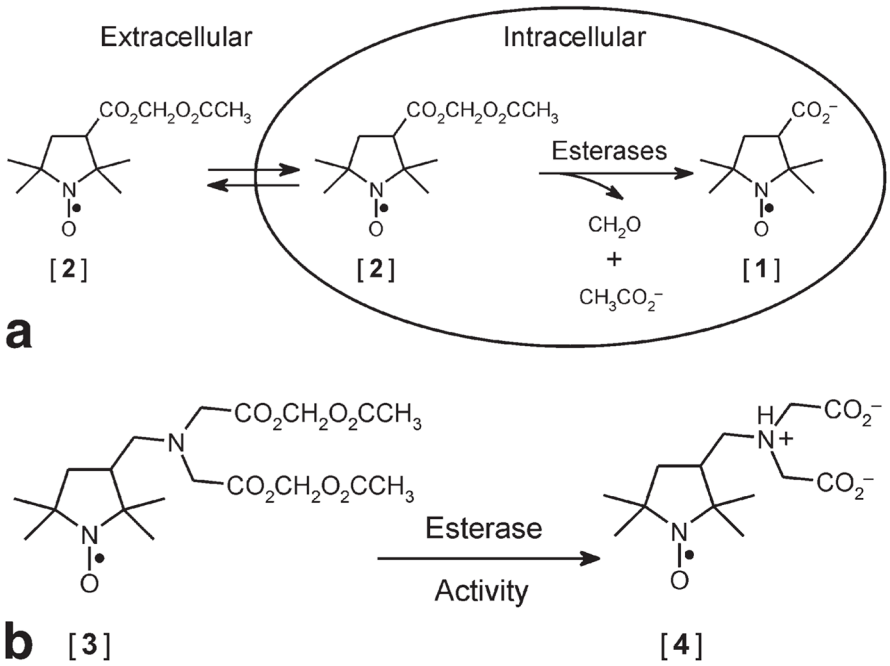

FIG 1.

a: Esterase-assisted accumulation of nitroxide [1] into cells. Membrane-permeant nitroxide AM ester [2] traverses the cell membrane and is hydrolyzed by intracellular esterases to the impermeant nitroxide [1], which becomes trapped. **b:** Structures of nitroxides [3] and [4]. The membrane-permeant nitroxide AM ester [3] and its intracellular hydrolysis product nitroxide [4], which is better retained in cells than nitroxide [1].

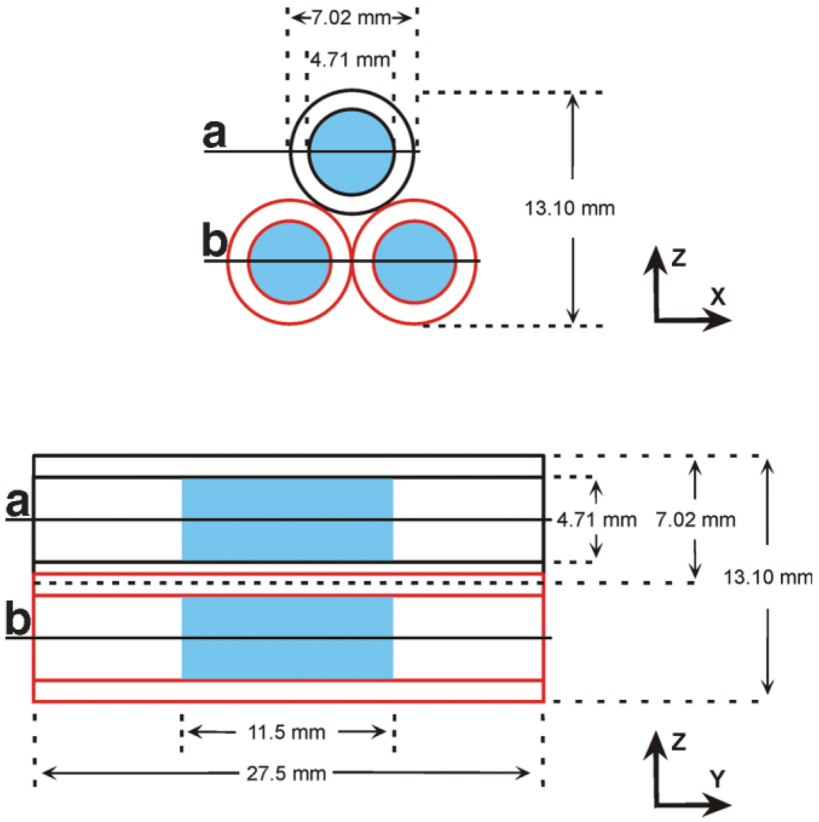

FIG 2.

Schematic representation of three-tube imaging phantom. The X-Z cross section shows the equilateral triangular arrangement of the tubes, with relevant dimensions indicated. The Y-Z projection view shows the same dimensions in addition to the length of each tube. Space occupied by the imageable sample is marked in blue. Lines A and B mark the approximate locations of the X-Y sections shown in Fig. 5b.

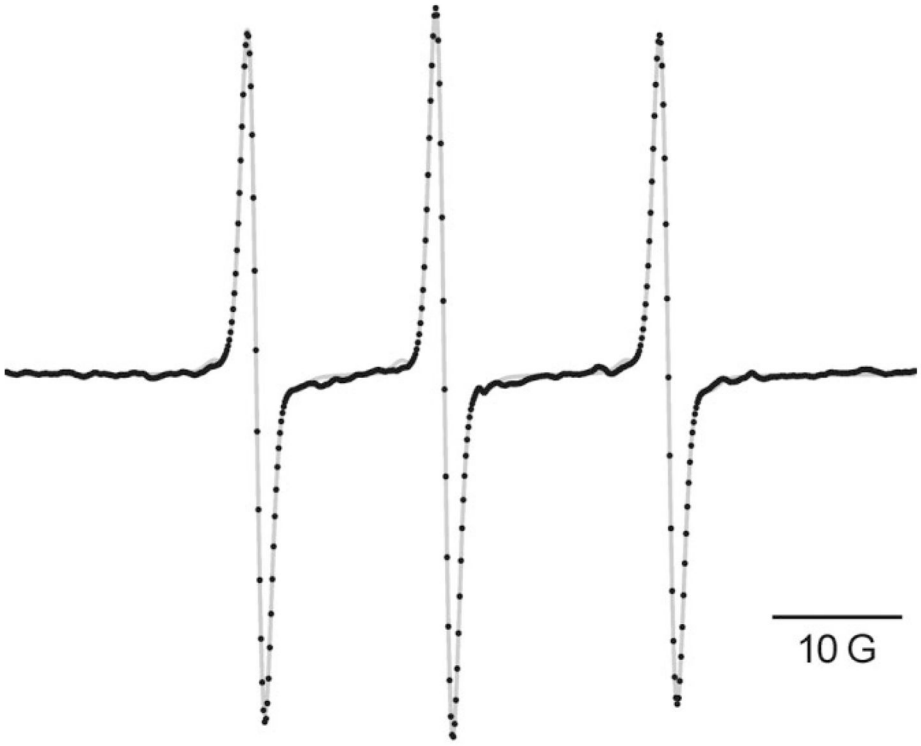

FIG 3.

EPR spectrum of 200 μM nitroxide [4] recorded at an operating frequency of 264.4 MHz. The instrumental parameters were: power, 1 mW; resonator Q value, 271; modulation frequency, 5.01 kHz; modulation amplitude (peak-to-peak), 0.05 mT; sweep interval, 10 mT, digitized with 1024 points at 30 ms dwell time per point; lock-in time constant, 30 ms. The digitized spectrum (black dots) is the average of 160 scans; the gray curve is the simulated spectrum generated with the algorithm of Robinson et al. (20).

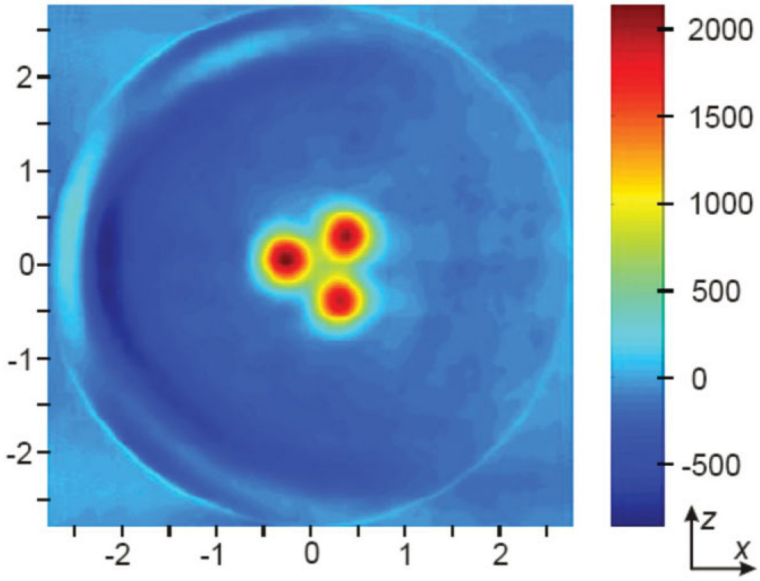

FIG 4.

EPR image of phantom filled with nitroxide [4] solution. Each tube was filled with 200 μl of a 200 μM solution of nitroxide [4]. The image was reconstructed from data obtained by taking one spectral projection along each of 99 azimuthal angles in the X-Z plane.

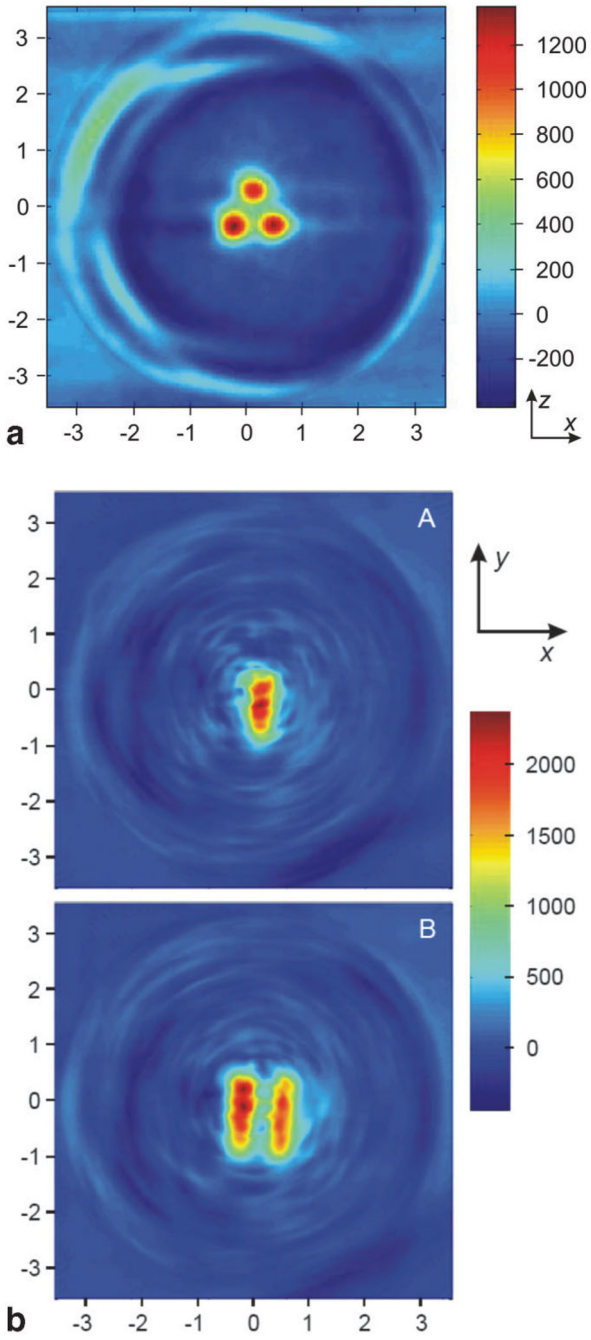

FIG 5.

EPR image of phantom containing cells with nitroxide [4] entrapped intracellularly. Each tube was filled with 2.6×10^7 lymphocytes that had been loaded with nitroxide [4] by incubation with nitroxide [3]. A 3D reconstruction was performed on a set of scans of 100 total projections (10 polar angles, each with 10 azimuthal angles). **a:** An X-Z section through the 3D reconstruction. **b:** Two X-Y sections (labeled A and B) through the 3D reconstruction. The approximate locations of the X-Y sections within the phantom correspond to locations marked by lines A and B in FIG. 2.